Vol.67: e24230842, 2024
https://doi.org/10.1590/1678-4324-2024230842
ISSN 1678-4324 Online Edition

BABT
Brazilian Archives of Biology and Technology

*Article - Engineering, Technology and Techniques*

# CRDN: Cognitive Radio with Deep Network for Proficient Spectrum Sharing in Massive MIMO Systems

**Vinoth Kumar Kalimuthu**[1*]
https://orcid.org/0000-0002-8920-4936

**Madhan Krishnamurthy**[2]
https://orcid.org/0009-0000-7758-1681

[1]Vivekanandha College of Engineering for Women (Autonomous), Department of ECE, Thiruchengode, India; [2]Anna University Regional Campus, Department of ECE, Madurai, Tamilnadu, India.

Editor-in-Chief: Alexandre Rasi Aoki
Associate Editor: Alexandre Rasi Aoki

Received: 09-Aug-2023; Accepted: 08-Jan-2024

*Correspondence: vinodkumaran87@gmail.com; Tel.: +919787367067 (V.K.K.).

**HIGHLIGHTS**

- CRNs are to effectively utilize the limited spectrum by pooling the available frequencies with other networks.
- To maximize the CR coverage and the average sum rate of the transmission in CRN mMIMO.
- Reducing deep learning rate and batch size, highestAASR achieved in our proposed model.

**Abstract:**The basic objective of cognitive radio networks (CRNs) are to effectively utilize the limited spectrum by strategically exploiting the unoccupied bands of frequencies or by pooling the available frequencies with other networks. The two approaches that have the potential to boost spectral efficiency of next-generation wireless communication networks are massive multiple-input multiple-output (mMIMO) and CRN. In this paper, we proposed a novel spectrum sharing technique for cognitive radio with mMIMO system using 3D space data gathering and learning based on Deep Learning method. Newfangled layer architecture is designed to train the primary network information assemblage named as Deep Learning Based Environment Training (DeepEnvNet). Also using mMIMO structure in cognitive radio base station (CRBS), we angular facts of CR user equipment (UE) by utilizing the spatial resolution of CBS. Iterative Hard Thresholding (IHT) can be used for direction of Arrival (DoA) estimation. The main 3D space spectrum coverage is accomplished via contemplation of two CBS for each cell in the network at the process of spectrum prophecy. Once the spectrum sensing is performed via DeepEnvNet, the greedy spectrum scheduling is performed via the two strategy: to maximize the CR coverage, to maximize the average sum rate of the transmission in CRN mMIMO. The experimental results are analyzed with the metrics of Average Achieved Sum Rate (AASR) and Average Scheduling Number (ASN). As reducing deep learning rate and batch size, highest AASR achieved in our proposed model than the earlier works of CRN spectrum sharing.

**Keywords:** Cognitive radio networks; Massive multiple-input multiple-output; Iterative Hard Thresholding.

## INTRODUCTION

Cognitive Radio (CR) has been viewed as an auspicious technique for enhancing the utilization of scarce radio spectrum resources for impending wireless communications and hand held device computing, given the explosive growth of wireless applications. It was first thought that CR, developed by Mitola [1] from software defined radio (SDR), would increase spectrum deployment. Radio emission regulations and the

utilization of radio spectrum resources are overseen by the Federal Communications Commission (FCC). Spectrum is increasingly in demand as new wireless applications emerge.

To increase spectrum utilization, the FCC has thought of making the licensed spectrum accessible to unlicensed users. Dynamic spectrum access enables unlicensed users to sense which parts of the spectrum are available, choose the best channel, coordinate access to spectrum channels with other users, and leave the channel when a licensed user shows up by taking advantage of the spectrum in an opportunistic manner. Future wireless networks can be referred to as cognitive radio networks (CRNs), which is in line with Haykins' description of CR [2].

A structure that is composed of several self-sufficient agents that work together to complete certain tasks either individually or in groups is known as a multiplex agency systems (MAS) [3, 4]. In order to meet the growing demand for wireless broadband connectivity and to address the issue of licensed spectrum being underutilized, cognitive spectrum sharing has recently been researched. These procedures can be broadly divided into three categories: interweave, underlay, and overlay [5]. Time-domain, frequency domain and space domain based spectrum access is implemented with the cooperation of SU and PU actions [6]. SUs frequently have fixed or limited sites free from interference from other broadcasts that are in progress [7]. MIMO and OFDM working together have recently attracted a lot of attention [8, 9].

In this work, we proposed a novel 3D space spectrum sensing for the cognitive radio system with massive MIMO using Deep Learning mechanism. Additionally, the couples of cognitive Base stations are considered to support the monitoring and spectrum analyzing of primary users and assist the CR users to effectively utilize the spectrum bands of cognitive radio. The 2D SBEM channel model for massive MIMO is modeled and estimated the channel propagated signal in the 3D space of CR. DoA estimation is also one of the major factor in the data gathering of PU with corresponding mMIMO channel of 3D. IHT based angular information prediction can be perform. Greedy Scheduling with two case of decision with either to coverage maximum users or maximum sum rate.

The remaining of the paper is prearranged as keep an eye on, Section II earlier developments on CR spectrum management are discussed and Section III describes the Design, methodology and mathematical modelling of proposed deep learning spectrum sensing of 3D. In Section IV, we present experimental results for the system, followed by a discussion on performance comparison of the previous implementations with our projected algorithm. Finally, Section V accomplishes this paper.

## LITERATURE SURVEY

In Cognitive Radio (CR) networks, Spectrum Sensing (SS) is crucial for determining the availability of frequency resources. The columnist gave a full analysis of current SS for CR advances in [10], both interference and endurance perspectives when it comes to a complete duplex functioning modes., and discussed the usage of knowledge techniques to improve SS performance while considering instances that utilize regional and multilateral sensing. Aside from that, [10] presents contemporary Spread spectrum protocol that is used in many real life applications like CR-based Internet of Things and Wireless Sensor Networks, as well as its possible significance during the frequency reservation, and the deployment of CR will continue into 5th Generation and subsequent generations.

The contributor of [11] offers two innovative strategies to deal with the problem of channel status prediction interweaving CRNs. The Hidden Markov Model (HMM) is used by both protocols. The given data is used in the training stages of both techniques to create a pair of HMM models: an actively functioning and a stand-by HMM version. Combining the two facsimiles yields the two-model HMMIn the first protocol, the prediction phase makes use of the Bayes theorem and the two state method of HMM, whereas the two stage method of HMM-SVM protocol makes use of the parameters produced by the 2-model HMM and the Support Vector Machine (SVM). In terms of accuracy, false-negative prediction probability, and true percentage, the HMM-SVM based two state method accomplishes healthier compared to classical HMM and 2-model HMM.

Future research into the likelihood for conflict across many different communication technologies will be essential, the spectrum of Radio frequency is going to be distributed among many devices, including radar and cellular systems [12–13]. The increased investments in infrastructure, particularly in technologies like LTE Advanced and 6G Technology, can help to a limited extent in reducing this problem. The columnist in [14] undertaking a handheld Volte systems of communication and nearby radar MIMO, a projection research on spectrum sharing has been conducted. Different intrusion passages are divided by mobile LTE communication systems and radar multiple input multiple output. The detected radar signal was projected into null space by the author of [14], who also demonstrates how to eliminate all meddling of the radar's several inputs, who chose the channel of interference with the best free channel. Insolent jammer attacks in massive MIMO cognitive radio network to loosen the spectrum effectiveness are discussed in [15]. To

overcome this effect [16], with the application of two cognitive Base Stations (CBS), improving the spectrum management using full space utilization of angular spread data.

## METHODOLOGY

The proposed system is modelled as CR network, Primary Network (PN) with massive MIMO with couple of CBS. The complete block diagram of the work is shown in Figure 1. Topology of the CRN with mMIMO antennas CBS and single antenna CRs is created. PR also considered with half duplex communication. The channel model we are taken is 2D Spatial Basis Expansion Model (SBEM). Once the network is formulated, the angular information gathering using IHT to estimate the DoA. Angular spread and PR network status congregation can be achieved by using our novel deep learning architecture of DeepEnvNet. Finally the greedy scheduling is performed to make spectrum sharing in 3D space for highest CRs.

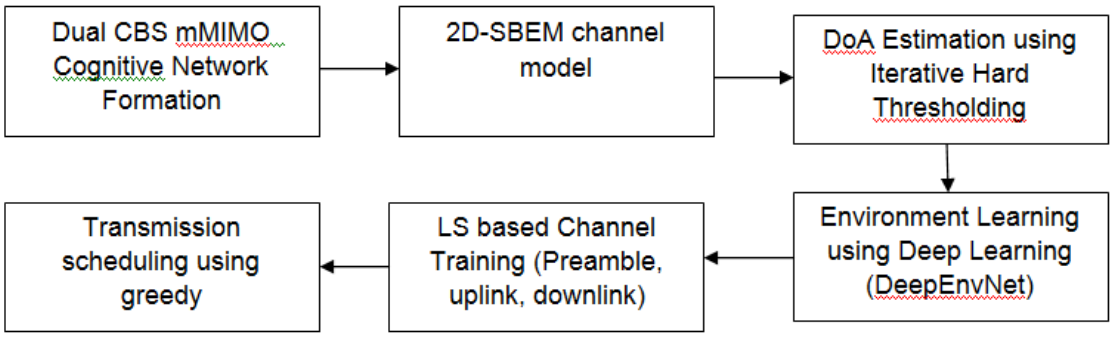


**Figure 1.** Block Diagram of Couple CBS based 3D space Spectrum Sharing

### System Model

Let contemplate a 3D space cognitive radio network with two CBS and N CR Users are dispersed at random throughout the cell's 3D environment. as shown in Figure 2. The position of CR-UE denoted as $X_N$, $Y_N$, $Z_N$. Each CBS is fortified with $T_x$ x $R_x$ antennas of uniform rectangular array (URA) [17]. $T_x$ is transmit antennas and $R_x$ is receive antennas of massive MIMO. CR-UE reserved with single antenna of uniform linear array (ULA) and it is mentioned as $CE_1$, $CE_2$,……., $CE_N$.. At the same time, we make the assumption that PU1 and PU2, half-duplex mode PU the transceiver couple, occasionally exchange messages with one another.

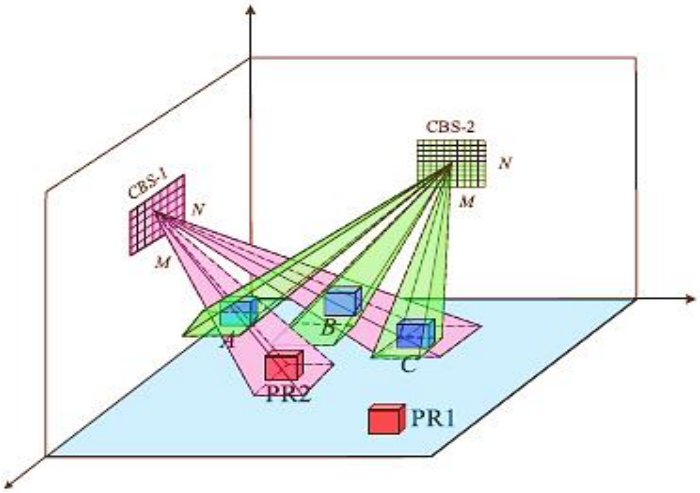


**Figure 2.** 3D Space dual CBS system

Besides, the wavelength is denoted as $\lambda$, and the inter-antenna spacing of both elevation and horizontal directions is denoted as $d_s$ which is set to be half of the $\lambda$ as shown in Figure 3. We assume that the signal transmitted from each CRs/PUs arrives to the CBS via $P_i$ clusters, each of which contains an assortment of distinctive resolvable pathways with associated elevation and azimuth DoA angles [18]. Additionally, $\theta_p$ $and$ $\Delta\theta_p$ are used to signify the average and orientation scatter (AS) of the vertical DoA angle of the p-th cluster, respectively. In the same way, the notations$\phi_p$ $and$ $\Delta\phi_p$, respectively, stand for the mean and AS of the horizontal DoA orientation of the p-th cluster.

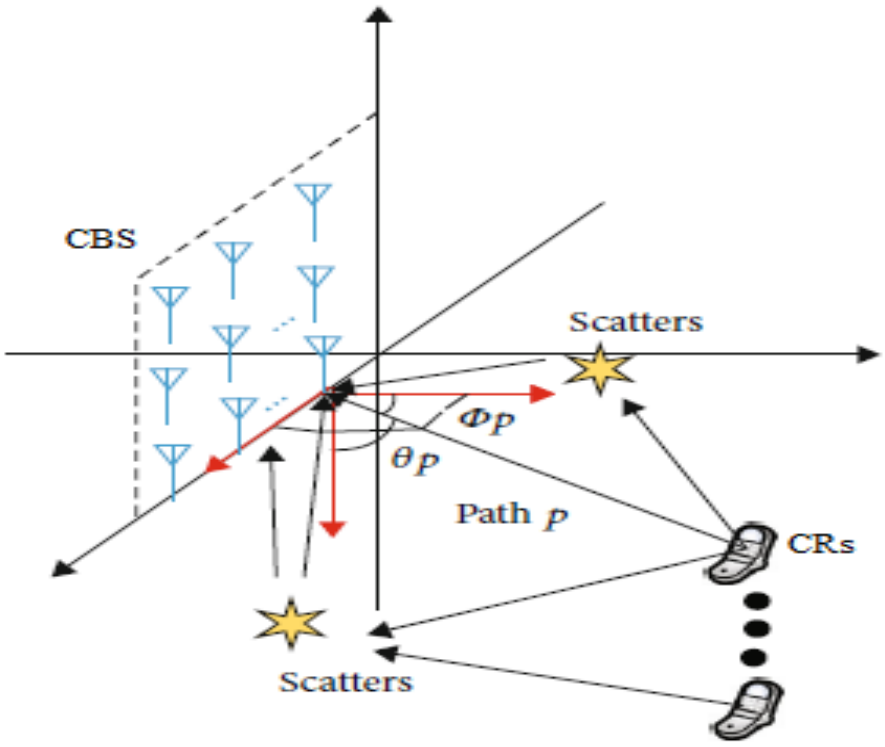


**Figure 3.** mMIMO system with rectangular antennas at the CBS.

The channel can be constructed through incorporating across the angular region as the signal passes through the p-th cluster.

$$\mathbf{H}_p = \int_{\theta_p-\Delta\theta_p}^{\theta_p+\Delta\theta_p} \int_{\phi_p-\Delta\phi_p}^{\phi_p+\Delta\phi_p} \beta(\theta,\phi)\, a(\theta) b^T(\theta,\phi) d\theta d\phi \quad (1)$$

where $\boldsymbol{H}_p$ stands for the channel matrix that makes up the p-th cluster incorporates.

$$\beta(\theta,\phi) = |\alpha(\theta,\phi)| \exp\{-j\phi(\theta,\phi)\} \quad (2)$$

Where, $\alpha(\theta,\phi)$ is the offsetting and $\phi(\theta,\phi)$ is the primary phase. $a(\theta)$In addition the array manifold vectors (AMVs) are $b^T(\theta,\phi)$ , that are expressed as,

$$a(\theta) = \left[1, e^{jX\cos(\theta)}, \ldots, e^{jX(M-1)\cos(\theta)}\right]^T \quad (3)$$

$$b(\theta,\phi) = \left[1, e^{jX\sin(\theta)\cos(\phi)}, \ldots, e^{jX(N-1)\sin(\theta)\cos(\phi)}\right]^T \quad (4)$$

Where

$$X \triangleq 2\pi\left(\frac{d}{\lambda}\right) \quad (5)$$

Next, a direction-finding matrix is defined and designated as $A(\theta,\phi) = a(\theta) b^T(\theta,\phi) \in \mathbb{C}^{M\times N}$ on the basis of AMVs, that are stated as,

$$A(\theta,\phi) = \begin{bmatrix} 1 & \cdots & e^{jX(N-1)\sin(\theta)\cos(\phi)} \\ e^{jX\cos(\theta)} & \cdots & e^{jX(\cos(\theta)+(N-1)\sin(\theta)\cos(\phi))} \\ \vdots & \vdots & \vdots \\ e^{jX(M-1)\cos(\theta)} & \cdots & e^{jX((M-1)\cos(\theta)+(N-1)\sin(\theta)\cos(\phi))} \end{bmatrix} \quad (6)$$

Based on above equation, the p-th cluster channel in equ(1) is able to be interpreted as,

$$\boldsymbol{H}_p = \int_{\theta_p-\Delta\theta_p}^{\theta_p+\Delta\theta_p} \int_{\phi_p-\Delta\phi_p}^{\phi_p+\Delta\phi_p} \beta(\theta,\phi)\, A(\theta,\phi) d\theta d\phi \quad (7)$$

Each of the clusters can be treated as a separate path, with the first-order contemplation factors and the line-of-sight (LOS) forming each path [19]. As a result, equ(7) can be rewritten as

$$\mathbf{H_p} = \beta\left(\theta_p,\phi_p\right) A\left(\theta_p,\phi_p\right) \quad (8)$$

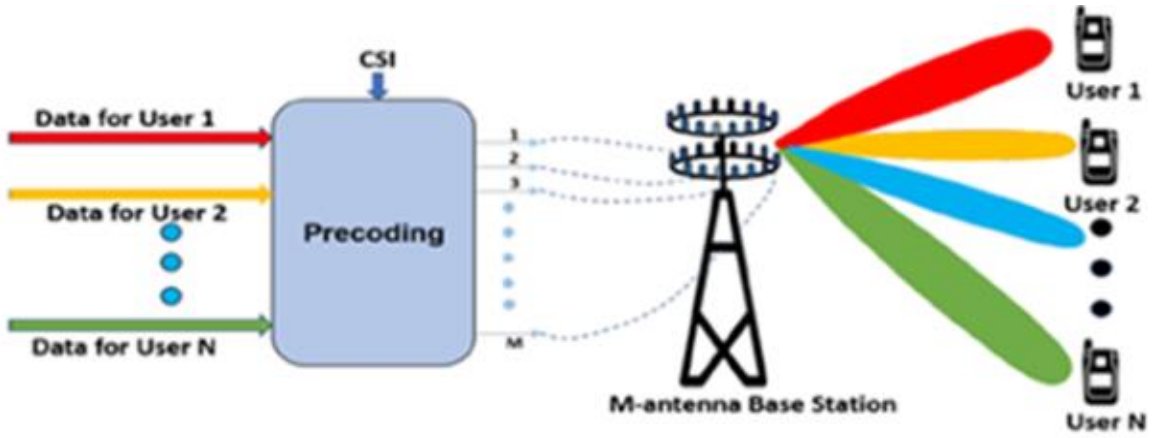


**Figure 4.** Massive MIMO Transmission

Following that, as seen in Figure 4, the communications signals received at the base station is expressed as:

$$Y_k = \sum_{i=1}^{U} \sum_{p=1}^{P_i} \beta(\theta_{i,p}, \phi_{i,p})\, A\left(\theta_{i,p}, \phi_{i,p}\right) x_{i,k} + W = \sum_{i=1}^{U} \sum_{p=1}^{P_i} H_{i,p} x_{i,k} + W \quad (9)$$

In which W is the Additive White Gaussian Random Noise framework, $x_{i,k}$ is the broadcast signal from $PU_i$, and k is the position of the received signal snapshot, and $H_{i,p} \in C^{M \times N}$ is the channel matrix for $PU_i$ on the p-th path. From (9), We understand that, for every single path p, just four attributes need to be calculated in order to recover the channel matrix, that are $\theta_{i,p}$, $\phi_{i,p}$, $\alpha\left(\theta_{i,p}, \phi_{i,p}\right)$ and $\phi(\theta_{i,p}, \phi_{i,p})$. Thus, the computational complexity of retrieving the parameters associated with the pathways is greatly lowered by contrasting with approximating variables in the original channel matrix.

**2D SBEM channel model**

The novelist of [20] projected a Discrete-Fourier-Transform-based spatial basis expansion model (SBEM) scheme to avoid pilot interference with channel sparsity than the earlier channel models [21].

To take advantage of a low-rank property with the goal of further lowering the degree of difficulty of channel estimation, 2D-SBEM is considered as channel model. Owing to the strong relationships between $a(\theta_{kp})$, p = 1, . . . , P, $h_k$ can be extended as follows from a perpendicular basis:

$$h_k = \sum_{q=1}^{v} k_q b_q \text{ ,for } k = 1,2,3\ldots,K \quad (10)$$

where $k_q$ are the equivalent coefficients and $b_q$ are basis vectors to be indomitable. Equ (10) is also acknowledged as BEM to predict uniform basis vectors $b_q$ for any possible $h_k$ [22]. At that time, the assignment of channel valuation will be significantly abridged and will be transformed to reckoning *v*coefficients$k_q$ only.

In order to use a smaller number of parameters to approximate the channel vector as

$$h_k = F^H h_k \approx [F^H]_{:,D_k} [\bar{h}]_{D_k,:} = \sum_{q \in D_k} \tilde{h}_{k,q} f_q \quad (11)$$

Where $\tilde{h}_{k,q} \triangleq [\tilde{h}_k]_q$ symbolizes the q-th element of $\tilde{h}_k$, and $f_q$ is the q-th column of $F^H$. Therefore, $D_k$ can be thought of as user-k's spatial signature. Relating with (10), the spreading out in (11) is also the underlying vectors $b_q$ and $f_q$ are perpendicular to one another in the field of BEM form. From now, the minimal BEM parameters are all that need to be estimated $\tilde{h}_{k,q}$. Remarkably, the directional vector and the DFT vector $f_q$ line up as $f_q = a(\theta_q)$where,

$$\theta_q = \arcsin\left(\frac{q\lambda}{Md}\right) \quad (12)$$

This indicates as a stacked beam is formed by $f_q$ in the path of the physical object. Hence, all beams $f_q$, $q \in D_k$ will be perpendicular to one another and pointing in the direction of user-k's AS [23].

**Iterative Hard Thresholding (IHT) based DoA Estimation**

Let the output of massive MIMO antenna arrays yt at time index t can be expressed as

$$y(t)=A(\theta)s(t)+n(t),\ t=1,2,3,\ldots.,N \quad (13)$$

Where N represents the total sample number and n(t) is the noise vector.$A(\theta)$ is the steering vector [24] articulated as

$$A(\theta)=[a(\theta_1),\ldots.,a(\theta_K)] \quad (14)$$

$$a(\theta_K)=\left[1,e^{\frac{j2\pi d\sin\theta_k}{\lambda}},\ldots..,e^{\frac{j2(M-1)\pi d\sin\theta_k}{\lambda}}\right]^T \quad (15)$$

T is the transpose symbol and $\theta_K$resembles to the DOA of kth source.

In this work, IHT algorithm [25] used to disentangle the sparse position of angle with number of repeatable process with:

$$S^{i+1}=H_k\left(S^{[i]}+\tilde{A}^H\left(Y-\tilde{A}S^{[i]}\right)\right) \quad (16)$$

Where $H_k(z)$is the non-linear function to nullifying the highest K rows of magnitude of $\bar{z}$.

$\bar{z}=[\|z_1\|_2,\ldots,\|z_{N\theta}\|_2]$, $\|z_k\|_2$symbolizes, $l_2$ normalization of k-th row of z. Take on that we have couple of roughly identical energy bases with DOA

$$[\alpha(\alpha+\Delta)](\Delta>0°) \quad (17)$$

The array output can be articulated as,

$$y(t)=S_1(t)a(\alpha)+S_2(t)a(\alpha+\Delta)+n(t) \quad (18)$$

The m-th element of $\hat{s}^{[1]}$at the first iteration, can be articulated as,

$$\hat{s}^{[1]}(m)=\sum_t\left|a^H(\theta_m)y(t)\right|^2=\left[a^H(\theta_m)y(t)\right]^H\left[a^H(\theta_m)y(t)\right]$$

$$=\sum_t[\langle\theta_m,\alpha\rangle^2 s_1^2(t)+\langle\theta_m,\alpha+\Delta\rangle^2 s_2^2(t)+2Ms_1(t)s_2(t)\langle\alpha,\alpha+\Delta\rangle+Mn_2(t)] \quad (19)$$

Here the $\langle\theta,\alpha\rangle$ denotes the inner product of $a(\theta)$ and $a(\alpha)$. Based on the equal energy denoted as below,

$$\sum\left|s_1(t)\right|^2\approx\sum\left|s_2(t)\right|^2 \quad (20)$$

Equ (20) assumption, when certain angle denoted as,

$$\beta(\alpha<\beta<(\alpha+\Delta)) \quad (21)$$

Certain angle [26] meets the below condition

$$\langle\beta,\alpha\rangle^2+\langle\beta,\alpha+\Delta\rangle^2>M^2+\langle\alpha,\alpha+\Delta\rangle^2=\langle\alpha+\Delta,\alpha\rangle^2+M^2 \quad (22)$$

At $\beta$ , the peak magnitude angle in $\hat{s}^{[1]}$ will be the refined DoA of estimation.

**DeepEnvNet: Environment training using deep learning**

In CRN, sensing of frequency band by hypothesis test for SU and PU [27]. The receiver output of i-th antenna is,

$$r_i(n)=h_i\times s(n)+\eta_{ci}(n) \quad (23)$$

where hi is the channel coefficient, s(n) is the primary received signal and $\eta_{ci}(n)$ is AWGN noise with $\eta_{ci}(n)\sim CN(0,\sigma_\eta^2)$. Thus, the CRN output $y_i(n)$ of the i-th antenna is given by [28],

$$y_i(n)=\frac{h_i^*}{|h_i|}r_i(n) \quad (24)$$

$$y_i(n)=\begin{cases}(\eta_i(n);H_0)\\ |h_i|\times s(n)+\eta_i(n);H_1\end{cases}=\begin{cases}\eta_i(n);H_0\\ s_i(n)+\eta_i(n);H_1\end{cases} \quad (25)$$

For CBSs to create the angle-based cognitive pre-coding of transmit beams, $Q_{i,PR1}$ and $Q_{i,PR2}$ must be known [16]. In order to prevent interference from the PR transmitter, CBS-1 might, for instance, route the incoming rays in the direction specified away from $Q_{i,PR1}$. In our work, angles of gathering of information are carried out using a deep-learning framework.

Deep learning is an approach to machine learning that makes use of layers of nonlinear processing units, each of which utilizes the outcome of the layer before it as inputs [29]. LSTM is sequence based deep learning architecture which we used here to propose our novel DeepEnvNet model for prediction of environment status with angular information.

LSTM is modified version of Recurrent Neural Network (RNN). RNN is recursive network modeled especially for processing sequential information using neural network concept in which dynamic performance of system is achieved via delay recursion in the network [30]. RNN is difficult to train long-term dependencies which leads to LSTM initialization. The architecture of the LSTM styles it an operative resolution to contest the disappearing gradient delinquent of the RNN as illustrated in Figure 5. LSTM blocks has four specific units which are Input gate, Output gate, forget gate, and the self-recurrent neuron as shown in Figure 5. These are the controlling units of LSTM memory.

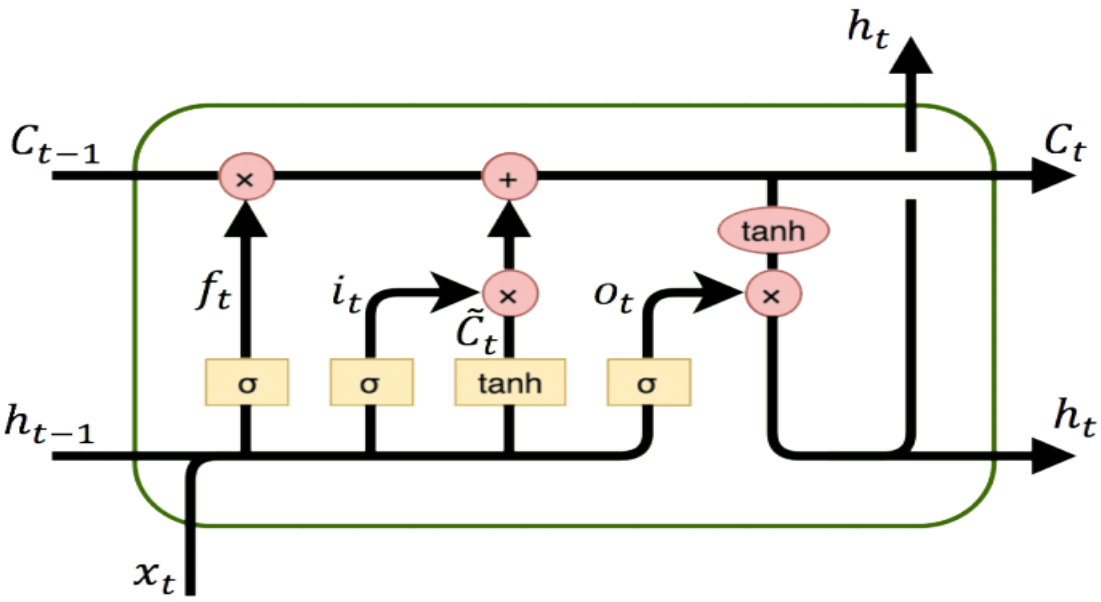


**Figure 5.** LSTM gate structure

The mathematical representation of each gate operations are mentioned as below,

$$f_t=\sigma\left(x_tU^f+h_{t-1}W^f+b_f\right) \quad (26)$$

$$i_t=\sigma\left(x_tU^I+h_{t-1}W^I+b_I\right) \quad (27)$$

$$o_t=\sigma\left(x_tU^o+h_{t-1}W^o+b_o\right) \quad (28)$$

$$\tilde{C}_t=\tanh\left(x_tU^c+h_{t-1}W^c+b_c\right) \quad (29)$$

$$C_t=C_{t-1}\otimes f_t\otimes i_t\otimes\tilde{C}_t \quad (30)$$

$$h_t=o_t\otimes\tanh(C_t) \quad (31)$$

Where b is biases, w is weights and U is the input weights, h is hidden, x is input and C is cell. Figure 6 shows the layer model of DeepEnvNet.

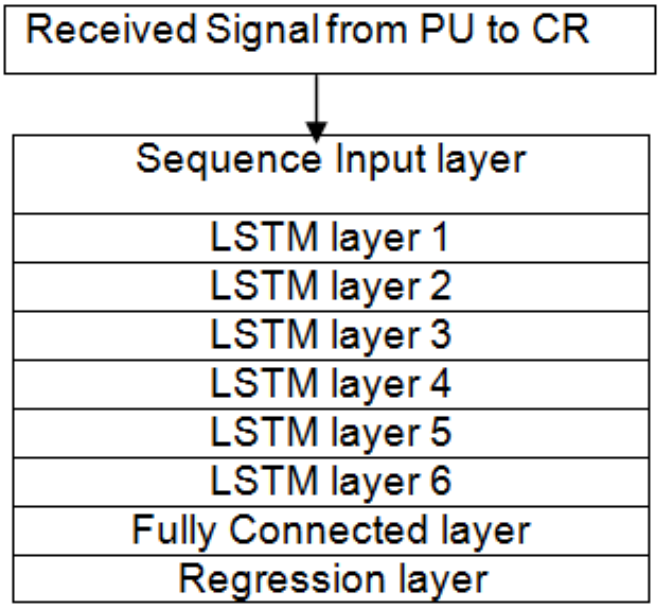


**Figure 6.** Proposed DeepEnvNet Layer Architecture

**Channel Learning**

The preamble, uplink training, and downlink training are the last three segments of the learning phase. An uplink preamble is used to gather each CR's degree characteristic before scheduling every single CR performs the uplink and downlink training intact on their angle signatures [31].

Direction of Arrival (DoA) Extraction with Preamble: For the purpose of to prevent contamination of the pilots, all CRs have been programmed to successively rerun a limited amount of orthogonal learning patterns when PR-link is identified to be inactive. Ten number of CRs will train after the other ten number of CRs have finished learning, for instance, if there are 20 CRs and only 10 orthogonal learning phases. This procedure, known as the prelude, may endure a little while lengthier. The traditional least square (LS) approach may then be used to determine the uplink channels of each CR endpoint, symbolized by $\widehat{H}_{i,k}, i = 1,2\ for\ k \in \kappa$. Alike toward (25), one can abstract $\hat{Q}_{i,k}$and evaluate $\hat{A}_{i,k}$from $\widehat{H}_{i,k}$, on behalf of each CR users.

On the rampage Pilot Contagion in learning of Uplink: Captivating the uplink preparation w.r.t. CBS-1 for photograph. Let us split the CRs hooked on $U^{tr}$assemblies and designate the listing segment of the $g$-th group as$\mathcal{U}_g$. It is prerequisite that CRs in the equivalent assembly do not have partly cover DoA signs, explicitly, $\widehat{Q}_{1,k} \cap \widehat{Q}_{1,s} = \emptyset$for $k, s \in \mathcal{U}_g$and $k \neq s$. We presume that the amount of assemblies is copious slighter than the CR quantity, i.e., $U^{tr} \ll |\mathcal{K}|$meanwhile$|\hat{Q}_{1,k}| \ll MN$. Let us apportion the similar orthogonal teaching series $x_g \in \mathbb{C}^{T_h \times 1}$ towards the whole thing CRs in the $g$-th assembly. Previously, CBS-1 may have received signals that were skewed into a matrix $Y_1 \in \mathbb{C}^{MN \times T_h}$as,

$$Y_1 = \sum_{g=1}^{U^{tr}} \sum_{k \in u_g} \mathrm{vec}(H_{1,k})\, x_g^H + Z_1 \quad (32)$$

Where $Z_1$is the additive white Gaussian noise function with zero mean. Channel estimated matrix of H from LS equalization algorithm as,

$$\mathrm{vec}\left(\widehat{H}_1^g\right) \triangleq Y_1 x_g \left(x_g^H x_g\right)^{-1} = \sum_{k \in u_g} \mathrm{vec}(H_{1,k}) + Z_1 x_g \left(x_g^H x_g\right)^{-1} \quad (33)$$

By applying the inverse vector process in equation (33), the final equalization matrix is returned by,

$$\widehat{H}_1^g = H_{1,k} + \sum_{s \in u_{g\{k\}}} H_{1,s} + Z_1^g, g = 1, \ldots., U^{tr} \quad (34)$$

Where $Z_1^g$ is AWGN noise function demarcated harmoniously from (33). $H_{1,s}$ is pilot contamination [31]. Extract its constituents inside $\hat{Q}_{1,k}$ as,

$$\lim_{M\to\infty}\lim_{N\to\infty}\frac{1}{\sqrt{MN}}\left[\hat{H}_{1,k}\right]_{\hat{Q}_{1,k}}=\lim_{M\to\infty}\lim_{N\to\infty}\frac{1}{\sqrt{MN}}\left[\tilde{H}_{1,k}\right]_{\hat{Q}_{1,k}}+\lim_{M\to\infty}\lim_{N\to\infty}\frac{1}{\sqrt{MN}}\left[\tilde{Z}_1^g\right]_{\hat{Q}_{1,k}} \quad (35)$$

The channel estimate $\hat{H}_{1,k}$ defined as,

$$\hat{H}_{1,k}=\left[F_M^H\right]_{:,\hat{Q}_{1,k}^{row}}\left[\tilde{H}_{1,k}\right]_{\hat{Q}_{1,k}}\left[F_N^H\right]_{\hat{Q}_{1,k}^{col},:} \quad (36)$$

Less Overhead based Learning of Downlink symbols: Just transmitted signal impulses that retrace the uplink pathway throughout downlink communication might reach CRs since the radio wave distribution path is reciprocal [32]. Commencing angle interchange property, we discern channel matrix $G_{i,k}$ can be correspondingly modeled as (8) departure angle DoD instead of DoA in uplink. Like the same angle signature also computed from uplink modelling. Hence $G_{i,k}$ can be stretched from 2D-SBEM given by,

$$G_{i,k}=F_M^H\tilde{G}_{i,k}F_N^H=\left[F_M^H\right]_{:,\bar{Q}_{1,k}^{row}}\left[\tilde{G}_{1,k}\right]_{\bar{Q}_{1,k}}\left[F_N^H\right]_{\bar{Q}_{1,k}^{col},:} \quad (37)$$

**Multi Objective Greedy Scheduling**

Considering the use of angle knowledge as well as the channel estimations discovered by channel retraining [33], we will examine the CR timing approach for transmitting information under various optimization targets.

Maximum Number of Scheduled CRs: Although the unplanned CRs are going to be reassigned to the following time frame, we will make every effort to maximise the total amount of CRs concurrently arranged by CBS-1 and CBS-2 in the initial time slot. Up until all CRs have been rescheduled for a minimum of one time, this procedure is going to be replayed. We suggested a straightforward greedy algorithm, and algorithm 1 encapsulates its key concepts.

Algorithm 1: 3D-SSS CR Scheduling using Greedy for P1
Assign: $\tilde{Q}_{i,t}$, $\tilde{Q}_{i,PR1}$, $\tilde{Q}_{i,PR2}$, $\Omega_{PR}$, $\Omega_{CR}$, for $k\epsilon$ Kand i = 1, 2; at begin n = 1 and the residual CR set $K_r = K$.
for n (time period)
assign $K_1(n) = K_2(n) = \emptyset$.
Pigeonhole the CRs within $K_r$ into $G_1, G_2, G_3, G_4$
set $K_r = K_r \backslash G_4$.
for any k
Compute the scheduling rate C(k)
Select k'= argmink C(k),
use $B(k') = 1\ or\ 2$ for CBS index
set $K_r = K_r \backslash \{k'\}$
if $B(k') = 1$
set $K_1(n) = K_1(n) \cup \{k'\}$
if $B(k') = 2$
set $K_2(n) = K_2(n) \cup \{k'\}$
Keep posted the states of enduring CRs
If G1, G2, G3 are all empty sets, go to next;
Else, go for next k.
Store $K_1(n), K_2(n)$ and the associate B(k) for their elements.
If $K_r \neq \emptyset$ , set n=n+1 and go to next n-th time slot;
Else, go to next
Set $U_{dd} = n$, output $K_1(n), K_2(n), n = 1, \ldots., U_{dd}$ as the final scheduling results.

Maximum Achievable Sum Rates: The following goal is to maximize the possible sum rates for every time slot beneath the given power constrictions. The detailed steps are shown in Algorithm 2.

Algorithm 2: 3D-SSS CR Scheduling using Greedy for P2

Assign: Input $\tilde{G}_{1,k}, \tilde{Q}_{i,t}, \tilde{Q}_{i,PR1}, \tilde{Q}_{i,PR2}, \Omega_{PR}, \Omega_{CR}$and average transmit power for $k \epsilon$ Kand *i*= 1, 2; at begin *n* = 1 and the residual CR set $K_r = K$.

for n (time period)

assign $K_1(n) = K_2(n) = \emptyset$.

Pigeonhole the CRs within $K_r$into $G_1, G_2, G_3, G_4$

set $K_r = K_r \backslash G_4$.

for any $kinG_1, G_2, G_3$

Calculate gain to schedule, as

$$\begin{cases} R\big(K_1(n)\cup\{k\},K_2(n)\big), & k\in G_1, \\ R(K_1(n),K_2(n)\cup\{k\}), & k\in G_2 \\ \max\{R\big(K_1(n)\cup\{k\},K_2(n)\big), & \\ \quad R(K_1(n),K_2(n)\cup\{k\})\} & k\in G_3 \end{cases} \tag{38}$$

Handpicked *k* with extreme sum-rate,

use $B(k') = 1\ or\ 2$ for CBS index.

set $K_r = K_r \backslash \{k'\}$

if $B(k') = 1$

set$K_1(n) = K_1(n) \cup \{k'\}$

if $B(k') = 2$

set$K_2(n) = K_2(n) \cup \{k'\}$

Keep posted the states of enduring CRs.

If $G_1$, $G_2$, $G_3$ are all empty sets, go to **next**;

Else, go for next k.

Store $K_1(n), K_2(n)$ and the associate *B(k)* for their elements.

If $K_r \neq \emptyset$ , set n=n+1 and go to next n-th time slot;

Else, go to **next**

Set $U_{dd} = n$, output $K_1(n), K_2(n), n = 1, \ldots., U_{dd}$as the final scheduling results.

## TESTING AND VALIDATION

To prove the efficiency of our proposed CR transmission via 5G massive MIMO in this section, we presented the simulated results of design with multiple scenarios. Table 1 shows some of the imperative considerations which are organized in the simulation environment of MATLAB 2020a. The performance of proposed DLSS is compared with the FSSS[16] and RS[34]

**Table 1.** Some of the important parameters for the simulation

| Coefficient | Value |
|---|---|
| Number of CR users | 12 |
| Number of PU | 3 |
| Area | 250m |
| Depth | 100m |
| Maximum Communication Distance | 50m |
| Number of Antennas of CBS | 128 with URA |
| Number of Antennas of CR | 1 with ULA |
| Antenna Element | Short Dipole Antenna |
| Carrier Frequency | 500 MHz |
| PU Transmission power | 0.1 W |
| Pathloss exponenet | 4 |
| Number of Symbols in each frame | 64 |
| Number of subcarriers | 128 |

The simulation environment of CR users, CR base station and primary users are positioned with the random distribution manner as shown in Figure 7. CBS1 and CBS2 are the two Base station which are taken at the sequent two sides of the cell region with location of CB1(100,250,100)and CBS2(250,100,100)which means two opposite sides of cell [35]. Three PU users are considered and denoted as PU1, PU2 and PU3. CR users are located in 12 distinct place with the x, y, z coordinates.

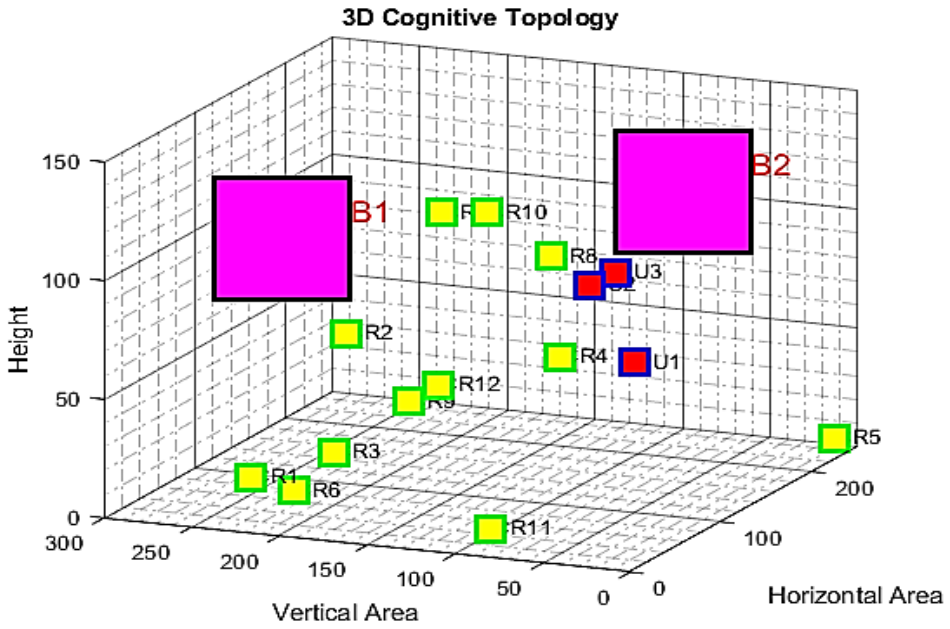


**Figure 7.** 3D space Cognitive Radio Topology

The way an antenna transmits electricity into the surrounding environment is described in three dimensions by its radiation pattern. The far-field, or the distance away from the antennas, is where this type of pattern is often measured. It may be described simply as the power emitted in a certain direction by a short dipole antenna. Figure 8 illustrates the radiation pattern of massive MIMO CBS.

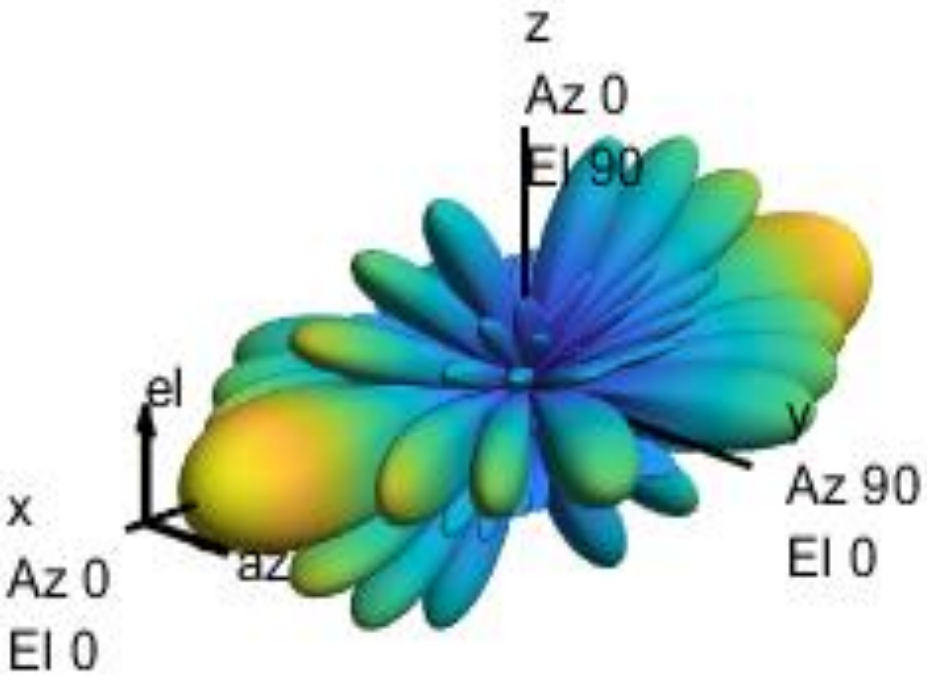


**Figure 8.** 3D radiation pattern of CBS URA antenna

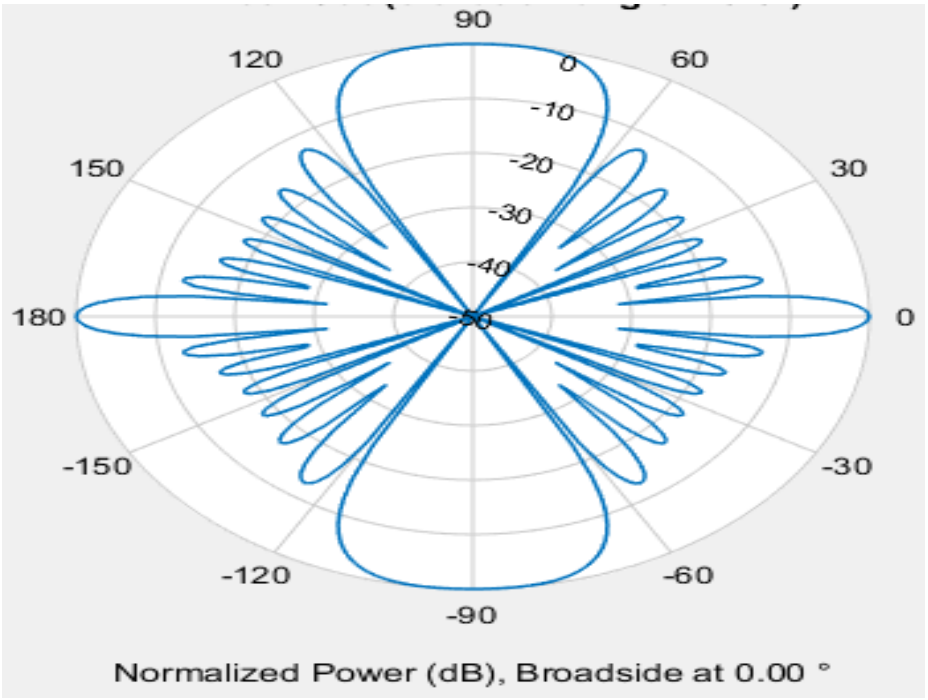


**Figure 9.** ULA 3-D radiation beam pattern

Figure 9 shows the beam pattern of single antenna CR users with ULA configuration.Figures 10 to 12 display the 2D spectrum of the arbitrary geometry null-spectrum function for several massive MIMO setups using 128 antennas from three PU users (SNR = 10 dB) with PU1-DoA of (10,50), PU2-DoA of (25,-22) and PU3-DoA of (28,1).

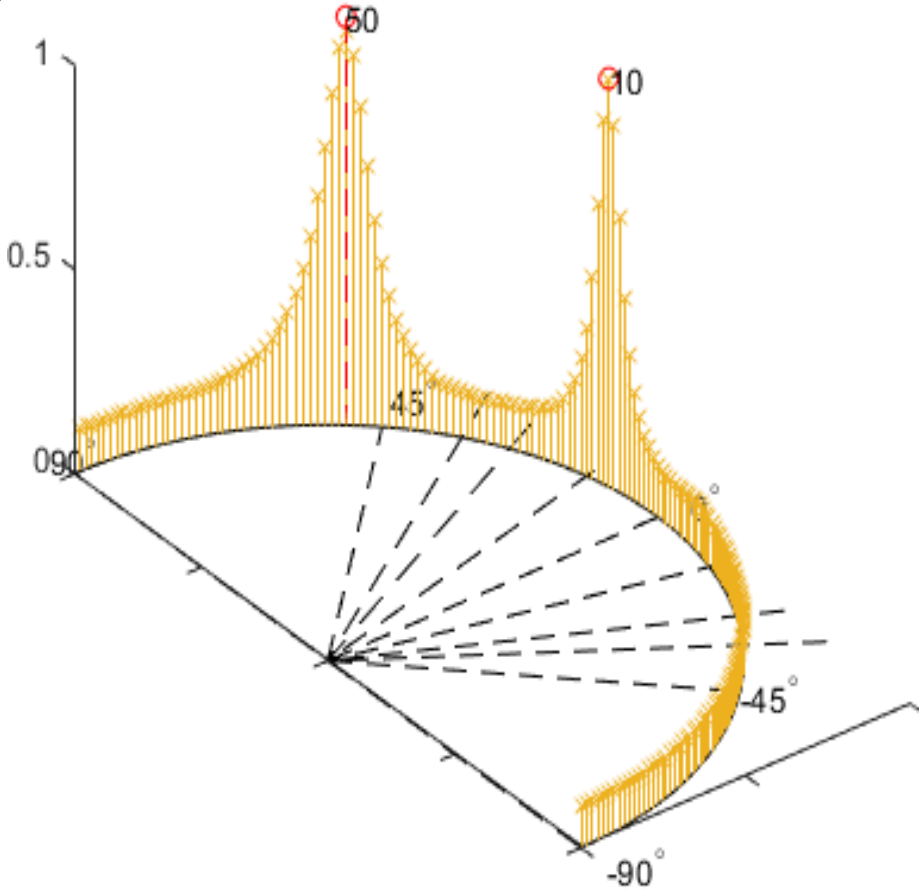


**Figure 10.** DoA of PU user 1 (10,50) estimated using IHT

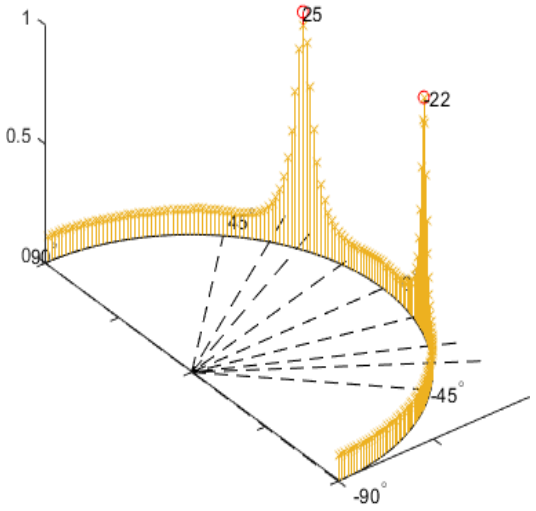


**Figure 11.** DoA of PU user 2 (25,-22) estimated using IHT

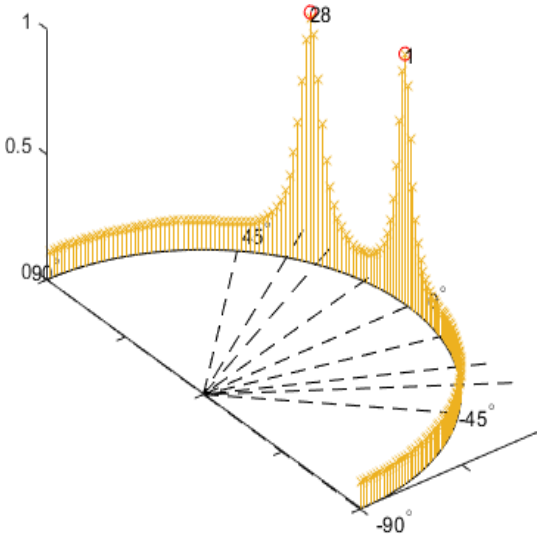


**Figure 12.** DoA of PU user 3 (1,28) estimated using IHT

Figure 13 shows the typical number of CRs scheduled by Algorithm 1 for single CBS/dual CBS situations per time slot. The maximum value of the dual CBS case is, however, roughly twice as high as the value of the single CBS case. Additionally, as the quantity of PR-links grows, the shielding effect gets more robust which means that, as expected, fewer CRs may be assigned each time period.

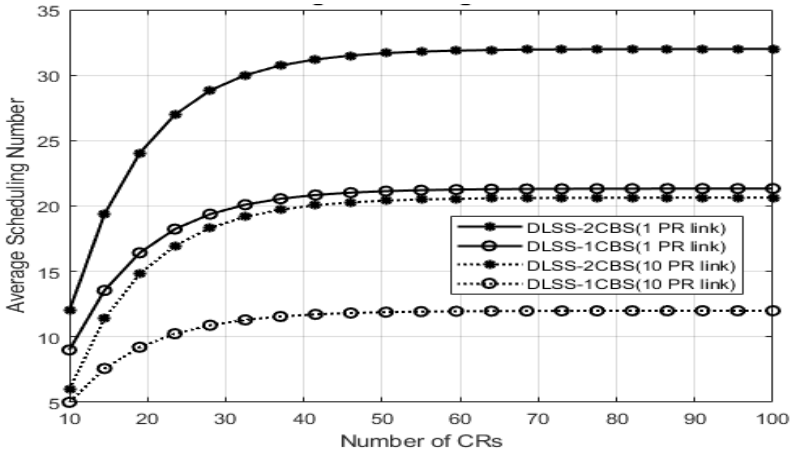


**Figure 13.** The mean of scheduled CRs of proposed DLSS with 1-CBS and 2-CBS

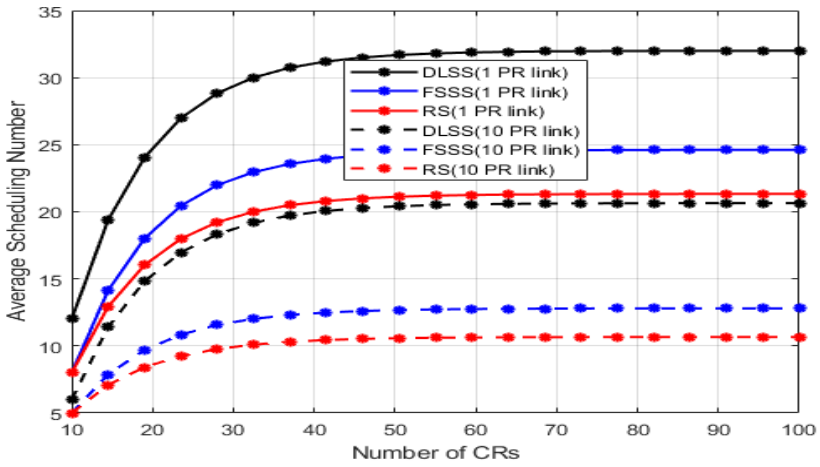


**Figure 14.** The mean of scheduled CRs for different PR link and methods

Scheduled user of CR in the proposed Deep Learning based Spectrum Sharing (DLSS) is 33 which is 32% higher than the earlier work of Full Space Spectrum Sharing (FSSS) and 57% higher than Random Scheduling (RS) method respectively as shown in Figure 14.In Figure 15, we illustrate the scheduling likelihood of each CR using Algorithm 1. Both the single CBS scenario plus the dual CBS scenario areanalysed when there are one or more PR-links. The ratio of the percentage of the amount of CRs which CBSs can schedule in relation to the overall amount of CRs is known as the scheduling likelihood. According to Figure 16, dual CBSs have a substantially higher scheduling chance than single CBSs do in every situation. Because a single PR may only block the view of one BS, the scheduling probability is 100% even though there is only one PR-link. Consequently, the suggested method can offer full-space covering within the cell. The scheduling chance of a single CBS, however, substantially decreases as the amount of PR-links upturns, whereas the setting up likelihood of dual CBSs remains advantageous.

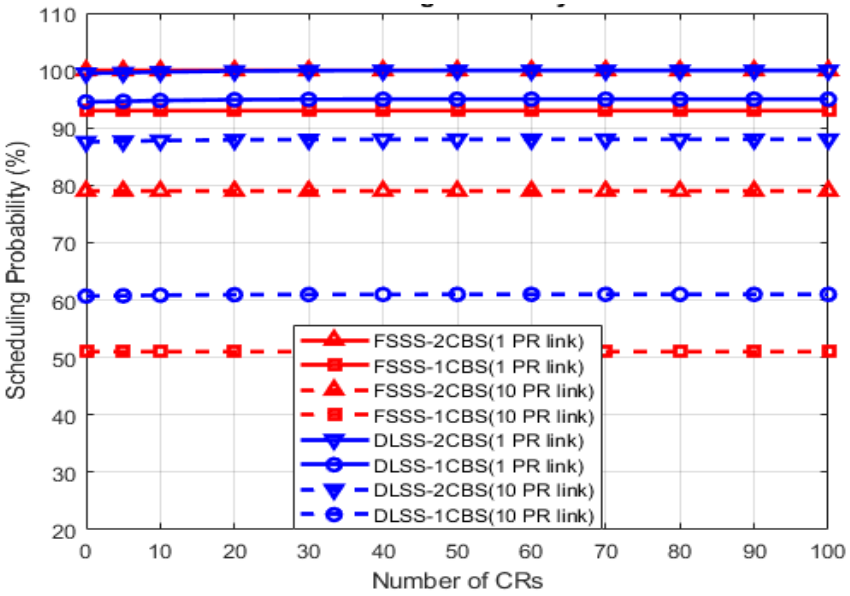


**Figure 15.** Probability Percentage of Scheduling

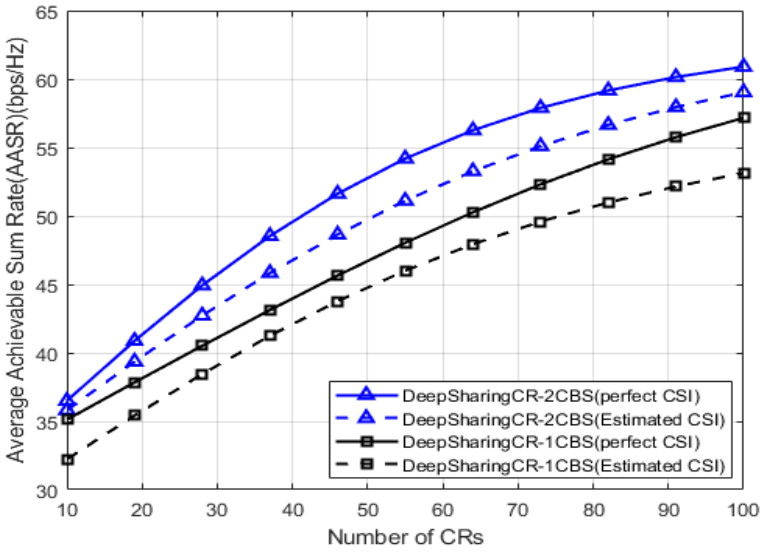


**Figure 16.** AASR of perfect and Estimated CSI for DLSS

The Average Achievable Sum Rates (AASR) of Alg 2 for the CBS-1/ CBS-2 instances, with faultless CSI and estimated CSI, are shown in Figure 16. When the overall number of CRs grows, so will the AASR attained by both situations. Despite this, the AASR for two CBSs is greater than one CBS, demonstrating the spectral management of the DLSS design and scheduling method. Owing to CE error, there is a considerable disparity between these two in both single and dual CBS scenarios. This break is not pretentious greatly by the quantity of CRs.

Figure 17 depicts the AASR from Alg 2 as a function of the important of each CR's DoA. K=100 is used to represent the entire quantity of CRs. when perceived in Figure 17, when |Qi,t | grows, the AASR attained by CBS-1 and CBS-2 situations diminishes. As ASR grows, so does the magnitude DFT spreads in $Q_{i,t}$, and each CR will inhabit a bigger DoA, which loosen the spectrum utilization via assignment to less users of CR.

The AASR and Average Scheduling number of CRs are listed out in Table 2 for Proposed DLSS method and compared it with the previous implementations of FLSS and RS algorithm. In this table the value of these metrics are shown for single CBS and dual CBS along with 1 PR link and 10 PR links. As we observed from this table AASR and scheduled CRs are improved 45% than the FLSS and 53% highest than the RS method respectively.

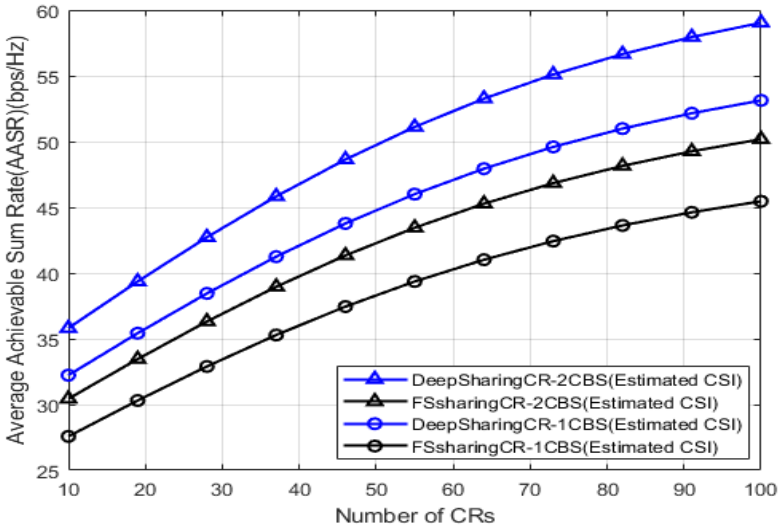


**Figure 17.** AASR of 1-CBS and 2-CBS for DLSS and FSSS

B is length of the steering vector, P is number of distint uncorrelated signals, L is snapshot number, k=4P which is largest singular value, $Q_e$ is number of samples in elevation and $Q_a$ is number of samples in azimuth. $J_{0=}$ $2Q_e$-1 and $J_{1=}$ $2Q_a$-1.

**Table 2.** AASRand Average scheduled CRs Comparison at number of CR at 40

| Algorithms | CBS | PR links | AASR (bps/Hz) | Average Scheduled CRs |
|---|---|---|---|---|
| DLSS | 1 | 1 | 54 | 31 |
| | | 10 | 51 | 20 |
| | 2 | 1 | 60 | 36 |
| | | 10 | 56 | 25 |
| FSSS | 1 | 1 | 45 | 24 |
| | | 10 | 39 | 13 |
| | 2 | 1 | 50 | 28 |
| | | 10 | 44 | 19 |
| RS | 1 | 1 | 41 | 21 |
| | | 10 | 36 | 11 |
| | 2 | 1 | 46 | 25 |
| | | 10 | 39 | 14 |

## CONCLUSION

Radio frequency spectrum is a restricted and valuable asset in wireless communication systems, and it has become a critical foundation for research and development activities in recent years. To solve spectrum scarcity and make the most of available spectrum, cognitive radio has emerged as a leading and advantageous technology. One of the critical components of cognitive radio is the ability to detect vacant spectrum possibilities. Among the approaches investigated thus far, energy detection has shown to be less difficult, practical, but sub-optimal. The performance of an energy detector for identifying spectrum holes was investigated in this work. We proposed a deep learning based 3D space effective spectrum sharing using improved sensing and decision methods. The simulation results are shown that, the proposed DLSS achieved the high AASR and average scheduled CRs than the earliest works FLSS and RS. For future work, we can implement the adaptive scheduling algorithm.

**Funding:** The authors declare they have no funding applied.
**Conflicts of Interest:**The authors declare they have no conflicts of interest to report regarding the present study.

## REFERENCES

1. Cebrail Ç, Musaab A.Evaluation of Eigenvalue and Block Diagonalization Beamforming Precoding Performance for 5G Technology over Rician Channel.TV-TG.2019;26(2):312-7. https://doi.org/10.17559/TV20170624224254.
2. Nasser A, Al Haj Hassan H, Abou Chaaya J, Mansour A, Yao KC. Spectrum Sensing for Cognitive Radio: Recent Advances and Future Challenge. IEEE Sens.J.2021;21(7):2408. https://doi.org/10.3390/ s21072408.
3. KhawarA,Abdelhadi A, Clancy TC. A mathematical analysis of cellular interference on the performance of S-band military radar systems. RG WTS.2014; 9–11.http://dx.doi.org/10.1109/WTS.2014.6835028.
4. VenkatramananM, ChinnaduraiM. Channel Estimation in MIMO TFT-OFDM Using Hybrid BESOA- CSOA Algorithms. TV-TG.2024;31(1):151-5. https://doi.org/10.17559/TV-20230502000598.
5. Junior MM, Guo B, Zhang C, Bai X. Interference Cancellation Based Spectrum Sharing for Massive MIMO Communication Systems. IEEE Sens.J. 2021; 21:3584. https://doi.org/10.3390/s21113584.
6. Fatemeh Zamanian S, Hossein Kahaei M, Mohammad Razavizadeh S, Svensson T. Attacking Massive MIMO Cognitive Radio Networks by Optimized Jamming. IEEE (OJ-COMS). 2021;2:2219–31. https://doi.org/10.1109/OJCOMS.2021.3114382.
7. Xie H, Wang B, Gao F. A Full-Space Spectrum-Sharing Strategy for Massive MIMO Cognitive Radio Systems. IEEE JSAC.2016; 34(10):2537-49. http://dx.doi.org/10.1109/JSAC.2016.2605238.
8. Cebrail Ç, FatihYavuzI.Studentized Extreme Eigenvalue Based Double Threshold Spectrum Sensing Under Noise Uncertainty.TV-TG.2020;27(2):353-7. https://doi.org/10.17559/TV-20170429133247.
9. Yin R, Zhou X, Qi W, Wu C, Cai Y. Grouping-Based Channel Estimation and Tracking for Millimeter Wave Massive MIMO Systems.Hindawi,Wirel.Commun.Mob.2021;1-14. https://doi.org/10.1155/2021/2922359.
10. Wang A, Yin R, Zhong C. Channel estimation for uniform rectangular array based massive MIMO systems with low complexity. IEEE (TVT).2019; 99(99):1–12.http://dx.doi.org/10.1109/TVT.2019.2893938.
11. Yin R, Zhou X, Wang A, Zhong C, Wu C, Chen X. Adaptive channel estimation and tracking for URA-based massive MIMO systems. IEEE Access. 2020; 8: 54213– 24. http://dx.doi.org/10.1109/ACCESS.2020.2981396.
12. Noh S, Zoltowski MD, Sung Y. Love DJ. Optimal pilot beam pattern design for massive MIMO systems. IEEE (ACSSC) 2013; 2072–6.http://dx.doi.org/10.1109/ACSSC.2013.6810671.

13. Rathika Pacharpalayam,Dhamodhiran, Sivaraj,Dhandapani. Spectrum Estimation and Optimal Secondary User Selection in Cognitive Radio Networks.TV-TG.2023;30(6):1744-1752. https://doi.org/10.17559/TV-20230223000377.
14. Liu L, Li Y, Zhang J. DoA estimation and achievable rate analysis for 3D millimeter wave massive MIMO systems.2014 IEEE (SPAWC). 2014; 6–10.http://dx.doi.org/10.1109/SPAWC.2014.6941306.
15. Xie H, Gao F, Zhang S, Jin S. A Simple DFT-aided Spatial Basis Expansion Model and Channel Estimation Strategy for TDD/FDD Massive MIMO Systems.IEEE.Trans.Inf.Theory. 2016; 6. https://doi.org/10.48550/arXiv.1511.04841.
16. Vijay Anand J, Manoharan P. S, Jeyadheep Vignesh J, Varatharajan M, Rubina Sherin M.Spider Search Algorithms for MIMO System and Assessment Using Simatic PCS7.TV-TG.2021;28(4):1118-26. https://doi.org/10.17559/TV-20200513113443
17. Xia J, He K, Xu W, Zhang S, Fan L, Karagiannidis G K. A MIMO detector with deep learning in the presence of correlated interference. IEEE (TVT),2020; 69(4):4492-97. https://doi.org/10.1109/TVT.2020.2972806
18. Liu F, Wang J, Sun C, Du R. Spatial Differencing Method for DOA Estimation Under the Coexistence of both Uncorrelated and Coherent signals. IEEE Trans Antenna Propag.2012; 60(4):2052–62. http://dx.doi.org/10.1109/TAP.2012.2186216.
19. Veeramakali T, Jayashri S, Prabu S. Intelligent dynamic spectrum allocation with bandwidth flexibility in cognitive radio network. Springer Science CCJ, 2017;20(2), 1575- 86. https://doi.org/10.1007/s11227-021-03637-3
20. Ravì D, Wong C, Deligianni F, Berthelot M, Andreu-Perez J, Lo B, Yang GZ. Deep Learning for Health Informatics.IEEE(JBHI). 2017; 21(1):4-21.https://doi.org/10.1109/JBHI.2016.2636665.
21. Sahiner B, Pezeshk A, Hadjiiski LM, Wang X, Drukker K, Cha KH, et al. Deep learning in medical imaging and radiation therapy. Med Phys. 2019 ;46(1):e1-e36. https://doi.org/10.1002%2Fmp.13264.
22. Zhang Z, Wang X, Long K, Vasilakos AV, Hanzo L. Largescale MIMO-based wireless backhaul in 5G networks.IEEEWirel. Commun. 2015; 22(5): 58–66. http://dx.doi.org/10.1109/MWC.2015.7306538.
23. Bao H, Fang J, Chen Z, Li H, Li S. An efficient Bayesian PAPR reduction method for OFDM-based massive MIMO systems. IEEE Trans. Wirel.Commun..2016; 15(6):4183–95. https://doi.org/10.48550/arXiv.1511.09013.
24. WangY, Ye Z, Wan P, & Zhao, J. A survey of dynamic spectrum allocation based on reinforcement learning algorithms in cognitive radio networks. Springer.Artif.Intell.Rev.2021; 51(3): 493-506. https://doi.org/10.1007/s10462-018-9639-x.
25. Lin B, Gao F, Zhang S, Zhou T, Alkhateeb A. Deep learningbased antenna selection and CSI extrapolation in massive MIMO systems. IEEE Trans. Wirel. Commun, 2021;20(11):7669-81. https://doi.org/10.1109/TWC.2021.3087318.
26. Mirza H,AdrianaL,VlatkoL.Residual Block Error Rate Prediction for IR HARQ Protocol.TV-TG.2020;27(4):1071-6.https://doi.org/10.17559/TV-20181220161917.
27. Xu W, Gao F, Tao X, Zhang J, Alkhateeb A. Computer Vision Aided mmWave Beam Alignment in V2X Communications. IEEE Trans. Wirel. Commun, 2023;22(4):2699-714. https://doi.org/10.1109/TWC.2022.3213541.
28. Liao J, Zhao J, Gao F, Li GY. Deep Learning Aided Low Complex Sphere Decoding for MIMO Detection. IEEE Trans. Commun, 2022;70(12):8046-59.https://doi.org/10.1109/TCOMM.2022.3218630
29. Jayamathi A, Jayasankar T, Vinoth kumar K.Novel Selective Mapping with Oppositional Hosted Cuckoo Optimization Algorithm for PAPR Reduction in 5G UFMC Systems.TV-TG.2022;29(2):464-71.https://doi.org/10.17559/TV-20210524085655.
30. Lin B, Gao F, Zhang S, Zhou T, Alkhateeb A. Deep learning based antenna selection and CSI extrapolation in massive MIMO systems. IEEE Trans. Wirel. Commun, 2021;20(11):7669-81. https://doi.org/10.1109/TWC.2021.3087318.
31. Sun J, Zhang Y, Xue J, Xu Z. Learning to search for MIMO detection. IEEE Trans. Wirel. Commun, 2020;19(11), 7571-84. https://doi.org/10.1109/TWC.2020.3012785.
32. Sivadasan J ,WilljuiceIruthayarajan M.Tuning of Nonlinear PID Controller for TRMS Using Evolutionary Computation Methods, TV-TG.2018;25(1):105-11. https://doi.org/10.17559/TV-20170612090511.
33. Jiang Y, Gao F. Electromagnetic Channel Model for Near Field MIMO Systems in the Half Space. IEEE Commun. Lett, 2023;27(2):706-10. https://doi.org/10.1109/LCOMM.2022.3229445.
34. YaqiuP,Mingqi L.A Novel PTS Scheme for PAPR Reduction of Filtered-OFDM Signals without Side Information.TV-TG.2020;27(4):1305-10.https://doi.org/10.17559/TV-20191012142626.
35. Cho YJ, Kim KH, Woo JY, Lee KS, No JS, Shin DJ. Low-complexity PTS schemes using dominant time-domain samples in OFDM systems. IEEE Trans. Broadcast., 2017;PP(99): 1-6. https://doi.org/10.1109/TBC.2017.2662228.